Pergamon

PII: S0191-8141(96)00073-9

Journal of Structural Geology, Vol. 19, No. 1, pp. 1 to 14, 1997

0191-8141/97 $17.00 + 0.00

A fracture model for quartz ribbons in straight gneisses

PAULA MACKINNON and FRANK FUETEN

Department of Earth Sciences, Brock University, St Catharines, Ontario, Canada L2S 3A1

and

PIERRE-YVES F. ROBIN

Geological Sciences, Erindale Campus, University of Toronto, Mississauga, Ontario, Canada L5L 1C6

(*Received* 21 *April* 1995; *accepted in revised form* 20 *August* 1996)

Abstract—Polycrystalline composite quartz ribbons in straight gneisses of the Grenville Province are explained as dilatant quartz-filled fractures formed parallel to a strong preexisting gneissosity. The ribbons are thin (≤3 mm), but long and continuous and have straight and truncating contacts with bordering grains of other minerals. They are similar in morphology to polycrystalline ribbons interpreted in the literature as resulting from high strains. In contrast, little strain is required if the ribbons form as quartz-filled fractures. A monoclinic symmetry of the shapes of ribbons and inclusions can be explained by fracture interactions as they propagate. The symmetry is consistent with a late extensional, south-side-down sense of shearing, which has been documented elsewhere in the Grenville Province. © 1997 Elsevier Science Ltd. All rights reserved.

INTRODUCTION

Quartz ribbons are a common feature in deformed quartz-bearing rocks. The term 'quartz ribbon' is usually used to describe any elongate single quartz grain or any elongate polycrystalline aggregate of quartz (e.g. Wilson, 1975; Bouchez, 1977; Boullier and Bouchez, 1978; McLelland, 1984; Culshaw and Fyson, 1984; Mancktelow, 1987; Vauchez, 1980). Quartz ribbons can be classified by their morphology into two types: (a) elongate single quartz grain ribbons (Bouchez, 1977); and (b) polycrystalline composite ribbons (Boullier and Bouchez, 1978).

Polycrystalline composite ribbons seem to be more common and are composed of many quartz grains which form a ribbon-like aggregate that is one or more grains in width. Boullier and Bouchez (1978) subdivide composite ribbons into 4 types, on the basis of their internal morphology: shape, size and orientation of grains and subgrains. The ribbons discussed here are most similar to these authors' type B3. Type B3 ribbons form discrete folia, with large shape ratios $X > Y > Z$, and are typically one to two grains in thickness. In the XZ plane, quartz grains within the ribbons are sub-rectangular and range from equant to elongate, with quartz–quartz boundaries sub-perpendicular to the long boundaries of the ribbon. The quartz within the ribbons may have a strong crystallographic preferred orientation with c-axes clustering in the Y-direction of the fabric ellipsoid (Boullier and Bouchez, 1978, fig. 2b; Culshaw and Fyson, 1984; McLelland, 1984). Type B3 quartz ribbons have been observed in highly deformed quartzofeldspathic gneisses (Boullier and Bouchez, 1978; Culshaw and Fyson, 1984; McLelland, 1984).

All of these authors interpret the polycrystalline ribbons as resulting from extensive deformation of pre-existing quartz layers or aggregates. Boullier and Bouchez (1978) argue that the difference in grain and subgrain morphologies between their types B1 to B4 correspond to differences in temperature, strain rate and extent of post-tectonic annealing.

This paper describes type B3 ribbons (Boullier and Bouchez, 1978) observed in granulite- and amphibolite-grade quartzofeldspathic gneisses from the southwestern Grenville Province of the Canadian Shield (Fig. 2). One important feature of these ribbons is their straight contacts with bordering non-quartz grains (Figs 1a & b and 3) which strongly suggest that these grains have been truncated. On the basis of the evidence documented here, we present a new model for the origin of these ribbons in which fracturing parallel to the pre-existing rock foliation produces dilatant quartz veins that have undergone little strain after their formation.

GEOLOGICAL SETTING

The ribbons examined here occur in gneisses of the Central Gneiss Belt (CGB) and the Central Metasedimentary Belt boundary thrust zone (CMBbtz) in the southwestern Grenville Province (Fig. 2). The Grenville Province, the youngest part of the Canadian Shield, is considered to have been assembled from 1.35 Ga with final cratonization ca 1.0 Ga (Moore, 1986). In both the CGB and CMBbtz the gneisses occur both as highly strained tectonic thrust sheets and as discrete high strain units within tectonic domains (Fig. 2). In both the CGB and the CMBbtz, the dominant tectonic regime has been one of northwestward-directed ductile thrusting under upper amphibolite to granulite facies metamorphism (Nadeau and Hanmer, 1992; Hanmer and McEachern, 1992).

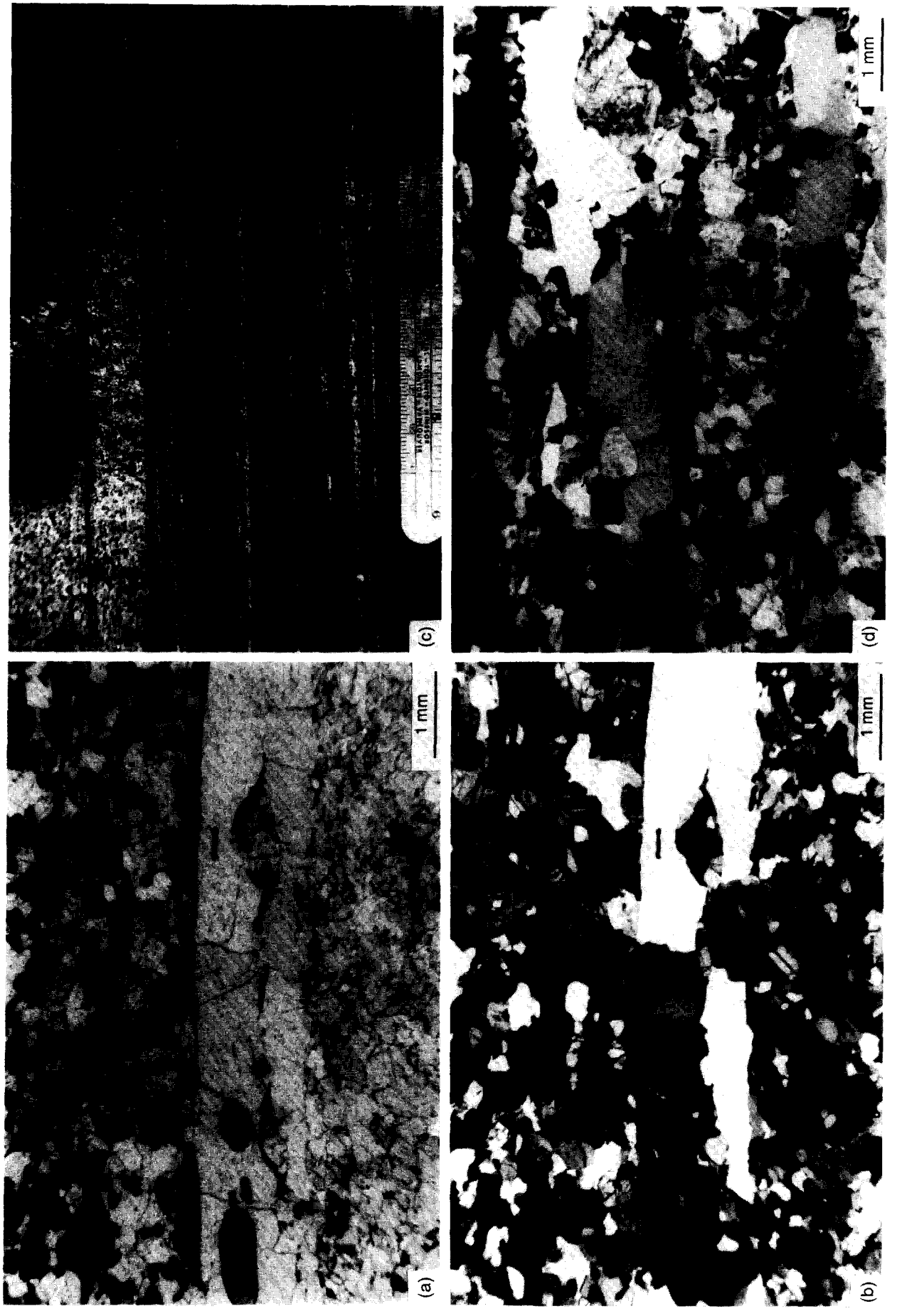
(c)
1 mm
(d)
1 mm
(a)
1 mm
(b)


1mm
(g)
1mm
(h)
1mm
(e)
1mm
(f)

The gneisses containing the ribbons have been described as straight gneisses (Hanmer, 1988a; Davidson *et al.*, 1982). They are S > L tectonites that are distinguished by the extreme continuity and regularity of their gneissic banding. The layer compositions range from quartzo–feldspathic to amphibolitic and all of the gneisses have reached upper amphibolite or granulite metamorphic facies.

Huntsville gneisses

The Huntsville thrust zone forms part of the Algonquin thrust stack of the Central Gneiss Belt. The thrust zone is a penetratively deformed thrust sheet, dipping shallowly southward, made up of thin interleaved sheets of fine-grained, flaggy, well lineated straight gneisses, mylonitic orthogneisses and highly strained metasedimentary tectonites. Southeast plunging extension lineations and shear-sense indicators are interpreted as the result of northwestward-directed thrusting (Nadeau and Hanmer, 1992). The metamorphic grade preserved in the Huntsville area ranges from granulite facies in the lower structural level of the thrust zone to upper amphibolite facies at higher structural levels in the zone (Nadeau, 1991). Geothermobarometric estimations of the peak metamorphic conditions range from 670°–830 °C and 7.7–10.5 kbars (Anovitz and Essene, 1990; Nadeau, 1991). Ribbony straight gneisses from the Huntsville thrust zone (Fig. 2, location A; UTM coords. 654300,5022250) are of upper amphibolite to granulite metamorphic grade. Compositions range from mafic to intermediate to felsic over distances of a mm or less across the gneissosity.

Mafic bands in the gneiss are defined by the assemblage (sample 89-10): hornblende + plagioclase + clinopyroxene + orthopyroxene + opaques ± biotite and the absence of K-feldspar and quartz.

Intermediate bands lacking hornblende, quartz or K-feldspar contain two main assemblages (sample 89-10) depending on their Ca to Al ratio:

(1) plagioclase + orthopyroxene (replaced by biotite) + biotite + opaques ± apatite, or, for higher Ca/Al,

(2) plagioclase + clinopyroxene + orthopyroxene + opaques + biotite.

Felsic bands in the gneiss lack hornblende, contain abundant quartz and K-feldspar, and have garnet. The felsic assemblage (sample 89-10) is: quartz + K-feldspar + plagioclase + garnet + opaques ± orthopyroxene (partially replaced by biotite ± chlorite) + biotite ± chlorite.

The clinopyroxene and orthopyroxene sometimes form polycrystalline ribbons in the mafic bands of the gneiss. The quartz ribbons described here occur primarily in the mafic bands or at boundaries between the mafic and felsic bands (sample 89-10). The gneissosity at the sampled outcrop undulates around large metagabbro boudins. Where the quartz ribbons are well developed the gneissosity strikes ENE and dips shallowly southeast (25°). The mineral extension lineation plunges shallowly to the WSW (2°) and is sub-parallel to the strike of the gneissosity. This is a local variation from the regionally developed down-dip SE plunging extension lineations. In outcrop the quartz ribbons weather to form resistant ridges which are often continuous for tens of centimetres (Fig. 1c).

CMBbtz gneisses

The CMBbtz forms the boundary between the underlying Central Gneiss Belt and the overlying Central Metasedimentary Belt of the Grenville Province. The boundary zone has been mapped as a major upper amphibolite facies ductile shear zone with northwestward-directed thrusting (Hanmer, 1988a). The thrusting has stacked successive southeast-dipping tonalitic and syenitic thrust sheets with tectonic marbles and metapelites. The straight gneisses both underlie and overlie less deformed gneisses that form the core of the identified thrust sheets.

The ribbony straight gneisses described here occur at the boundary between the Redstone and Dysart thrust sheets (Fig. 2, location B; UTM coords. 680603,4985068) and are overlain in the south by a marble mélange (Hanmer, 1988b). The gneisses have been mapped as granitic straight gneiss and dated at 1065 ± 15 Ma (Hanmer, 1988b; van Breemen and Hanmer, 1986). The granitic straight gneiss is really a composite gneiss composed of interlayered gneisses of three recognizable types, all of which contain ubiquitous quartz ribbons. The assemblage of this composite gneiss is: quartz + K-feldspar + plagioclase + hornblende + biotite ± clinopyroxene ± orthopyroxene ± muscovite ± calcite.

The interlayering of these different gneiss types contributes to the straight gneiss character of the out-

Fig. 1. All photomicrographs are of the *X–Z* plane, looking up toward the northwest for the Huntsville sample and up toward the southwest for the CMBbtz samples. (a) Photomicrograph (plane polarized light) of a quartz ribbon within the Huntsville gneisses with truncated pyroxene grains at the upper border (sample 89-10). Note the *S*-symmetry of polymineralic inclusions and elongate garnet inclusions. (b) Same view as (a) but with crossed polarizing filters. Note the subrectangular nature of the quartz grains within the ribbons and the slight undulatory extinction. The polymineralic inclusions lie on the long boundaries of the quartz grains in the ribbons. (c) Huntsville quartz ribbons in outcrop. White layers are quartz ribbons. The darkest layers are mafic layers. The intermediate coloured layers are intermediate layers and the light layers at the top of the picture are quartzofeldspathic felsic layers. Samples 89-5 and 89-6 shown in (d) to (h) are from the CMBbtz quartzo-feldspathic gneiss. (d) Photomicrograph of large quartz ribbons and quartz-free feldspar layers (sample 89-6). Note the hooked spur-like promontory of K-feldspar in the large quartz ribbon. (e) Elongate polymineralic inclusion of feldspar within a quartz ribbon (sample 89-6). Note the smooth sharp contacts of the inclusion with the surrounding quartz. To the upper right is a large K-feldspar with undulose extinction and core-and-mantle structure. (f) An *S*-shaped inclusion with long tails that link with other inclusions (sample 89-5). The feldspar in the upper half of the photo has a polygonal granoblastic texture with well-developed *Y*-shaped triple junctions. (g) An *S*-shaped inclusion with long tails (sample 89-6). (h) An *S*-shaped inclusion in a large quartz ribbon (sample 89-6). The inclusion occurs at a foliation-parallel quartz-quartz boundary. Note the spur-like promontories of feldspar. The plagioclase and K-feldspar are extensively sericitized in the upper half of the photo. The ribbon boundary at the bottom of the photo is scalloped.

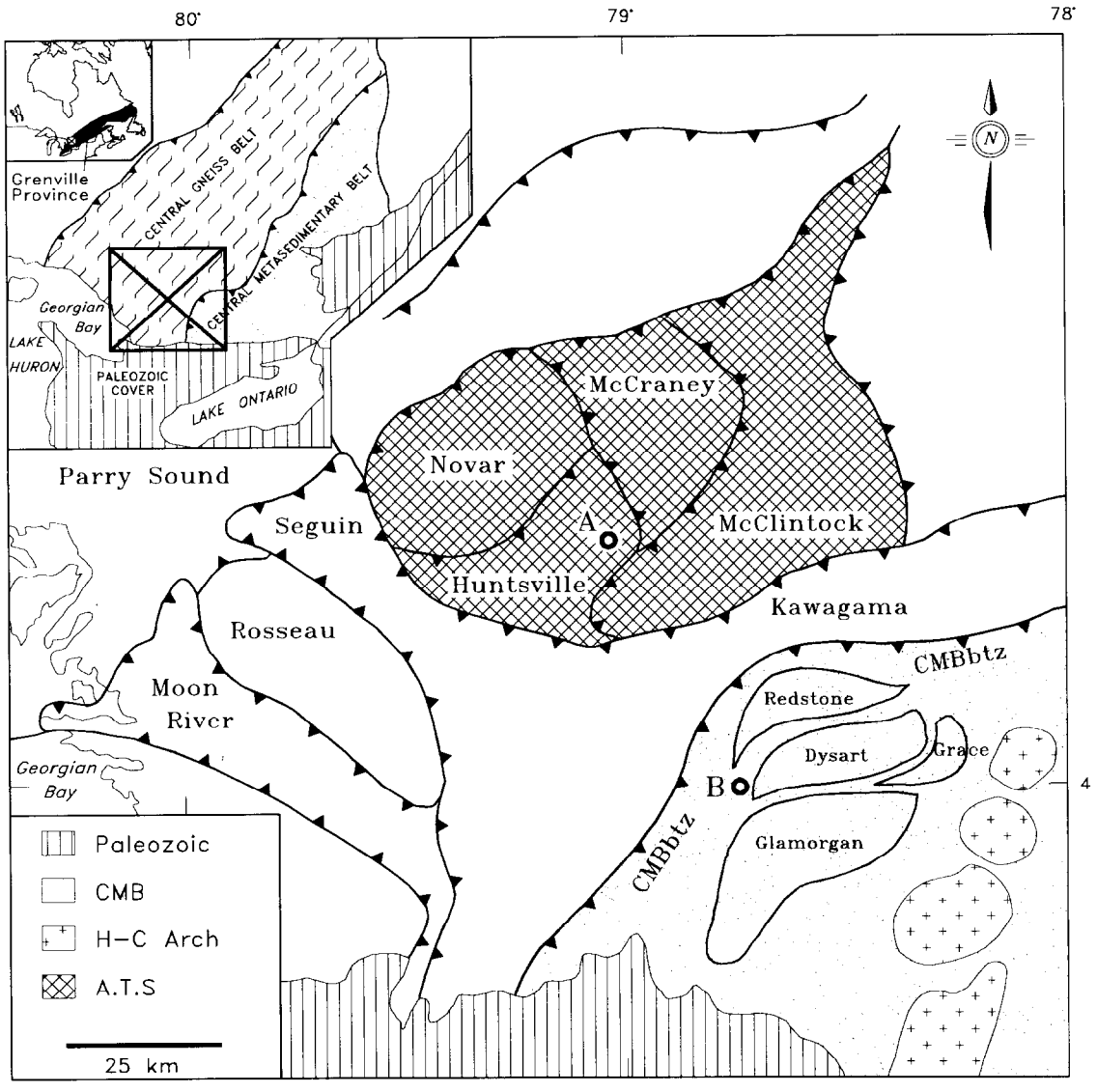

Fig. 2. Location of samples with quartz ribbons discussed in the paper. Location A is in the Huntsville thrust zone of the Central Gneiss Belt. Location B is in the Central Metasedimentary Belt boundary tectonic zone.

crop. The gneissosity at this outcrop strikes NNW and dips gently (10°) to the east. There is a mineral stretching lineation comprised of quartz and feldspar which plunges shallowly (2°) to the south and is almost parallel to the strike of the gneissosity.

Banded gneiss. The gneiss type with the best gneissic banding in the outcrop (samples 89-1, 89-2) consists of alternating pink quartzo-feldspathic (alkali-feldspar granite composition) layers and black amphibolitic (hornblende/biotite-rich syenite composition) layers (MacKinnon, 1994). The banded gneiss has a granoblastic texture with the exception of the polycrystalline quartz ribbons.

Clinopyroxene gneiss. A gneiss (samples 89-3, 89-5, 89-7) with less well developed internal layering forms large layers in the composite gneiss. It is quartzo-feldspathic in composition (granite to alkali-feldspar granite) with foliation traces formed by clinopyroxene, hornblende and occasional corroded orthopyroxene. This gneiss also has well developed polycrystalline quartz ribbons.

Quartzofeldspathic gneiss. The third gneiss type (sample 89-6) has no mafic component and is completely quartzofeldspathic. The quartzofeldspathic gneiss contains large (up to one cm) alkali-feldspar augen with partially recrystallized margins in a fine-grained, granoblastic alkali-feldspar matrix which is cut by large polycrystalline quartz ribbons which form the foliation.

A common aspect of both host gneisses described here is a strongly anisotropic fabric resulting from large deformations under granulite to upper amphibolite conditions. No cross-cutting or layer-parallel larger quartz veins were observed at either location.

PETROGRAPHIC FEATURES OF THE QUARTZ RIBBONS

The quartz ribbons discussed here are foliation-parallel, polycrystalline, and usually one grain diameter wide, with aspect ratios up to greater than 70:1 in sections parallel to the mineralogical lineation (*XZ* plane). In sections perpendicular to the lineation (*YZ* plane) the

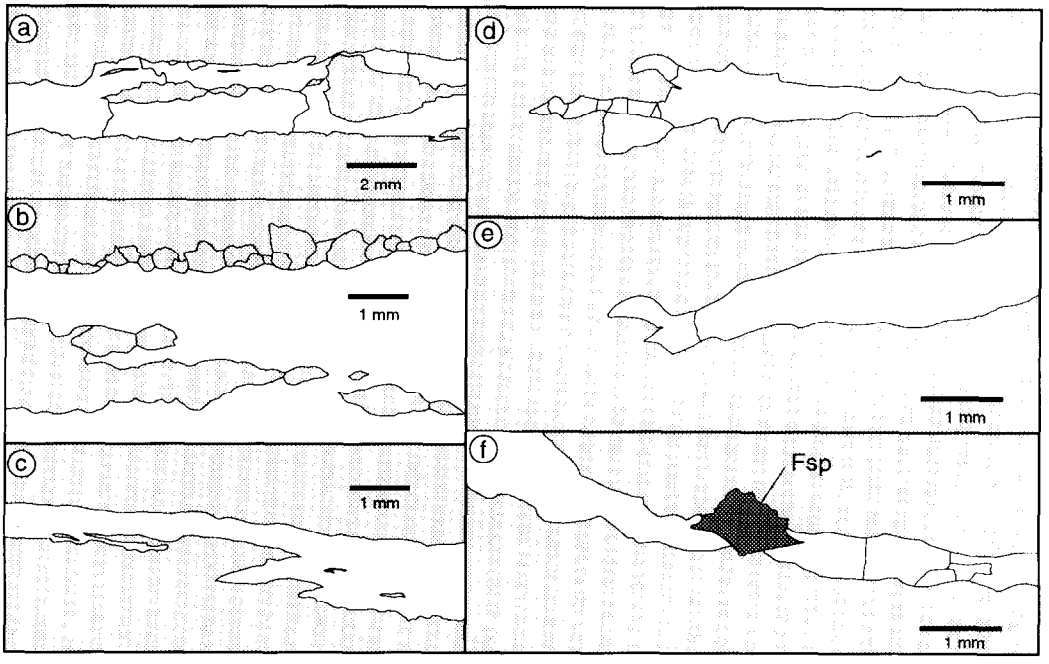

Fig. 3. Line drawings from photomicrographs of quartz ribbons (same plane and direction of viewing as Fig. 1). The white area is the ribbon quartz. Quartz–quartz grain boundaries are shown in (a), (d), (e) and (f). The light grey area is dominantly K-feldspar. All of the inclusions in the ribbons are K-feldspar. (a) Large quartz ribbon with rounded and slivered feldspar inclusions (sample 89-2). (b) Scalloped ribbon-quartz–feldspar grain boundaries (sample 89-6). Feldspar–feldspar grain boundaries at the upper ribbon boundary are outlined. Note the embayment of the quartz–ribbon feldspar grain boundary at feldspar–feldspar grain contacts. The same relationship can be seen at the boundaries of the feldspar inclusions. (c) A branching quartz ribbon with feldspar promontories (sample 89-5). (d) A branching ribbon termination with smaller quartz grains. (e) A branching spur-like termination of a quartz ribbon. (f) The terminations of two quartz ribbons at a K-feldspar grain (dark grey).

quartz ribbons also have high aspect ratios (20:1). The ribbons thus form folia rather than rods. Quartz grains within the ribbons are elongate (aspect ratio ~4:1) and have subrectangular sections, with grain boundaries subperpendicular to the long axes of the ribbons (Figs. 1b & 3a). The largest quartz grains within the ribbons occur in the centre where the folia attains its maximum thickness. The size and aspect ratio of quartz grains tends to decrease towards the terminations of the ribbons. Quartz within the ribbons exhibits some undulose extinction and subgrains.

Ribbon thicknesses range from about 0.3 mm to 3 mm. They account for a modal fraction of at least 30 %. Quartz ribbons may be several cm (or in the extreme case 10's of cm, see Fig. 1c) long. Large quartz ribbons usually extend across the entire thin section in sections cut parallel to lineation and their terminations are only rarely observed in thin section.

In general, regions adjacent to the quartz ribbons are virtually quartz-free although they may contain isolated, small, inequant quartz grains. In the quartzofeldspathic gneiss from the CMBbtz (sample 89-6), quartz ribbons alternate with quartz-poor layers consisting of equant, polygonal feldspar (Fig. 1d). This texture is also observed in some quartzofeldspathic layers in the clinopyroxene gneiss and in quartzofeldspathic layers in the banded gneiss. Quartz-poor feldspar (dominantly K-feldspar) layers between quartz ribbons range from several mm to less than 0.5 mm (one grain diameter) in width (Fig. 1d).

There is some minor sericitization of both plagioclase and K-feldspar in all the gneisses but it is more predominant in the CMBbtz quartzofeldspathic gneiss (Fig. 1e–h). In no case does the modal fraction of sericite exceed 2%. In the CMBbtz gneisses, some quartz ribbons are observed to wrap around large feldspar porphyroclasts. In two of the observed cases, the shape of the ribbons around the porphyroclast are not symmetric with respect to the trace of the foliation plane as observed in the X–Z plane (Fig. 4). For convenience, this monoclinic symmetry of the ribbon fabric is referred to as an asymmetry throughout the text. The sense of asymmetry is the same in both cases.

Ribbon boundaries

Boundaries along the long edges of ribbons range from straight (Fig. 1a & b) to arcuate (Fig. 1f) to scalloped (Figs. 1h & 3b) and form a distinct border between domains composed almost entirely of quartz and domains almost entirely devoid of quartz (Fig. 1d & e). Quartz ribbons are observed to have straight contacts with bordering clinopyroxene, orthopyroxene and feldspar grains, all of which have irregular shapes if they are entirely contained within quartz free domains (Fig. 1a). An occasional characteristic of the long-edge ribbon boundaries are scalloped contacts with bordering feldspar grains (Figs 1f & 1h and 3b). At scalloped contacts the deepest embayment of the quartz boundary often occurs at the feldspar–feldspar boundary between two neighbouring feldspar grains. The feldspar grains have convex contacts on both sides of a quartz ribbon. Some

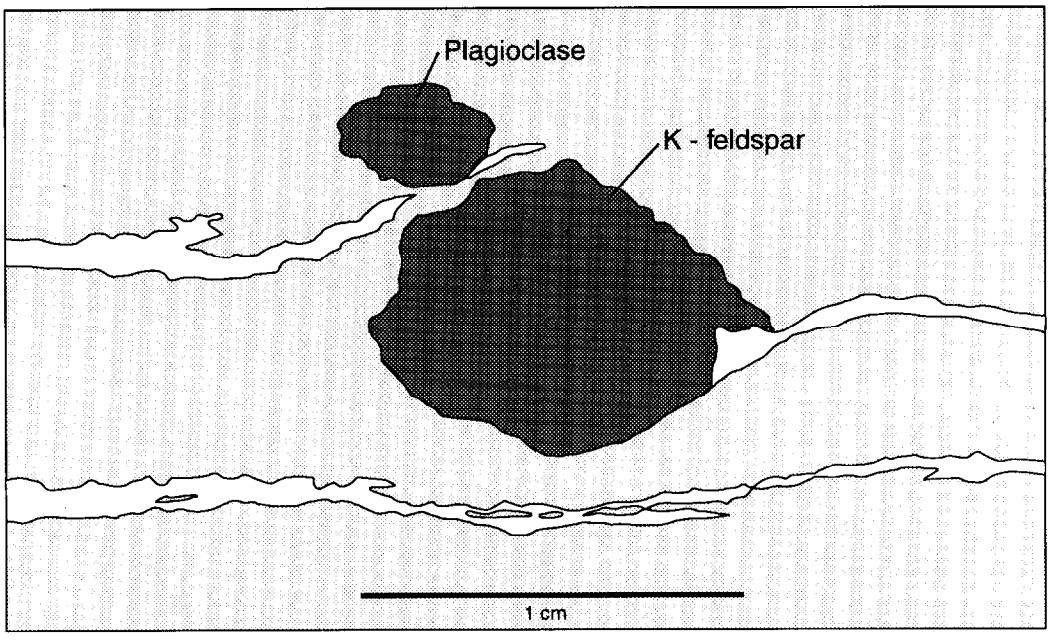

Fig. 4. Sketch from a photomicrograph (*XZ* plane, viewed in the same direction as in Fig. 1 (d)–(h), foliation parallel to scale bar) of quartz ribbons. Note the monoclinic symmetry of the deflection of the ribbons around the feldspar grain.

enclosed feldspar lenses within the quartz ribbons also exhibit these convex scalloped contacts (Fig. 3a & b).

Quartz–quartz boundaries within ribbons range from straight to moderately sutured. Most of the quartz–quartz boundaries are sub-perpendicular to the long boundaries of the ribbons (Fig. 1b & d). The quartz–quartz boundaries that are sub-parallel to the long ribbon boundaries are often localized along trails of mineral inclusions in the ribbons that parallel the long ribbon boundaries (Fig. 1b & h).

Quartz ribbons frequently end in branching terminations which may be sharp or blunt or consist of several smaller quartz grains (Fig. 3c–f) The branching terminations may involve larger feldspar grains (Fig. 3f) and leave spur-like terminations on single feldspar grains. The quartz ribbons may also branch and rejoin along their length. This produces spur-like promontories of feldspar in the ribbons or long lenses of feldspar contained within the ribbons (Figs. 1d & 3c).

Ribbon inclusions

The majority of quartz ribbons have inclusions of feldspar or other minerals. In the Huntsville gneisses the inclusion types may be monomineral garnet (majority), opaques, orthopyroxene, or biotite. Polymineralic inclusions are commonly garnet–orthopyroxene–plagioclase combinations ±biotite, ±clinopyroxene, and ±opaques. In the CMBbtz gneisses the inclusions are monocrystalline K-feldspar or plagioclase or polycrystalline K-feldspar and/or plagioclase. In all cases the mineralogy of the inclusions is the same as that of the adjacent matrix (Fig. 1a–b and e–h).

All inclusions are elongate parallel to the foliation and the long boundaries of the ribbon and range from nearly equant, with tails (Fig. 1a & h), to long narrow lenses (Fig. 1e–g). The matrix between two branching ribbons may thin to a feldspar promontory and to a string of inclusions as the ribbons merge. All of the inclusions have boundaries ranging from straight (Fig. 1e) to curved (Fig. 1a & f–h) to slightly scalloped (Fig. 3b). The foliation-parallel dimensions of grains within ribbons is similar to that of grains of the same mineral within the matrix. The long boundaries of the inclusions exhibit the same shapes as the external ribbon boundaries discussed above. In particular, the curvature of long inclusion trails never exceeds the curvature of the ribbon boundaries.

The majority of inclusions are symmetric about the foliation plane; some asymmetric inclusions can be identified as distinctly S or Z shaped. All asymmetric inclusions in both the CGB and CMBbtz ribbon gneisses have an *S*-symmetry when viewed in the *XZ* plane (looking NW at Huntsville: Fig. 1a–b; looking SW at CMBbtz: Fig. 1d–h). The regional shear sense in both areas has been interpreted as the result of northwestward-directed thrusting (Hanmer, 1988a; Nadeau and Hanmer, 1992). No convincing shear sense indicators were found in hand samples or at the outcrop in either area.

Preferred crystallographic orientation of quartz

Some of the quartz within the ribbons exhibits undulose extinction and subgrains (Fig. 1e). All of the ribbon quartz exhibits a strong preferred crystallographic orientation which was observed by insertion of a mica plate and subsequently confirmed by Universal-stage measurements. Quartz *c*-axis fabrics were measured for both ribbon quartz and non-ribbon quartz in selected samples. *C*-axis data are presented in the *XZ* plane of the fabric ellipsoid (Fig. 5). In the four samples from the CMBbtz, the *c*-axes form a peak distribution centred about the *Y* direction of the bulk fabric ellipsoid (Fig. 5). Both ribbon and non-ribbon quartz *c*-axes have this

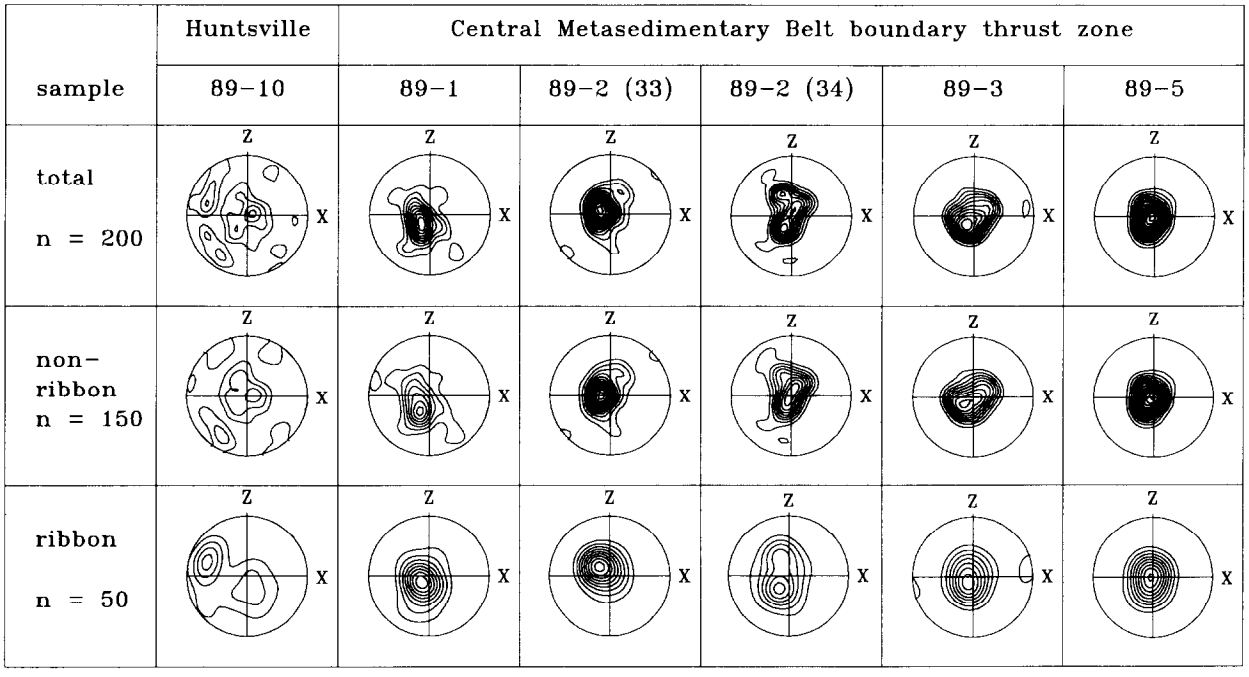

Fig. 5. Equal-area plots of quartz *c*-axes are presented in the *X*–*Z* plane, viewed in the same directions as given in Fig. 1 for Huntsville and CMBbtz. Data are contoured using a continuous Gaussian weighting function by the method of Robin and Jowett (1986). For each section, the *c*-axes of all quartz grains measured are presented in one plot and the *c*-axes of both ribbon and non-ribbon quartz grains are presented in separate plots.

distribution. The reproducibility of the fabric from one sample can be seen in sections 33 and 34 (both from sample 89-2) (Fig. 5). The sample from Huntsville has the maximum peak for the total *c*-axes at the *Y* axis orientation of the bulk fabric ellipsoid and a minor peak at an orientation midway between *X* and *Z* and perpendicular to *Y* (Fig. 5).

Summary of petrographic observations

The external and internal characteristics of these quartz ribbons can be summarized as follows. The external features of these ribbons, which are common to all 4 types of polycrystalline ribbons of Boullier and Bouchez (1978) are that they are large, have a high aspect ratio and are concordant with the foliation in the rock. These ribbons have straight or slightly scalloped boundaries, which appear to truncate grains adjacent to the boundaries. Ribbons branch, have feldspar promontories and trails of polymineralic and monomineralic inclusions. Inclusions exhibit consistent asymmetries. Common internal features of these ribbons are that the quartz within them exhibits a strong crystallographic preferred orientation which is similar to that of the quartz within the matrix.

A FRACTURE MODEL FOR QUARTZ RIBBONS

Existing models of ribbon formation (Boullier and Bouchez, 1978; Culshaw and Fyson, 1984) have generally attributed the straight boundaries to transposition by intense deformation. The strong crystallographic preferred orientation was attributed to intracrystalline glide and taken to confirm the intense strains (Boullier and Bouchez, 1978). These models cannot explain the presence of truncated grains at ribbon boundaries, the delicate elongate inclusions identical to thin slivers of matrix rock and the branching morphology.

The truncation of the bordering grains can most easily be explained as due to fracturing. The alternation of long thin lenses of feldspar with quartz ribbons is suggestive of some crack–seal textures (Ramsay, 1980). The branching and the curvature of ribbon terminations are similar to features commonly observed in dykes, produced in laboratory experiments with acrylic plastics, and interpreted in terms of fracture mechanics (Pollard *et al.*, 1982; Rogers and Bird, 1986; Olson and Pollard, 1989; Thomas and Pollard, 1993). For these reasons a fracture origin for the quartz ribbons is proposed. Mechanical anisotropies such as provided by gneissic layering or foliation are expected to constrain the location and orientation of the veins.

Vein-parallel dilatancy

It is proposed that the quartz ribbons formed as silica-filled fractures. Two end-member models can be envisaged which both produce silica-filled fractures parallel to the gneissic layering. In the first model, dilatant cracks form parallel to the layering (Fig. 6). The ribbon/vein grows by accretion along interfaces similar to the mechanism by which crack–seal veins develop (Ramsay, 1980). Sawyer and Robin (1986) have termed this mechanism 'vein-parallel dilatancy'.

Two possible origins for inclusions can be envisaged. In the first, two non-coplanar propagating quartz ribbons may interact and link to isolate inclusions

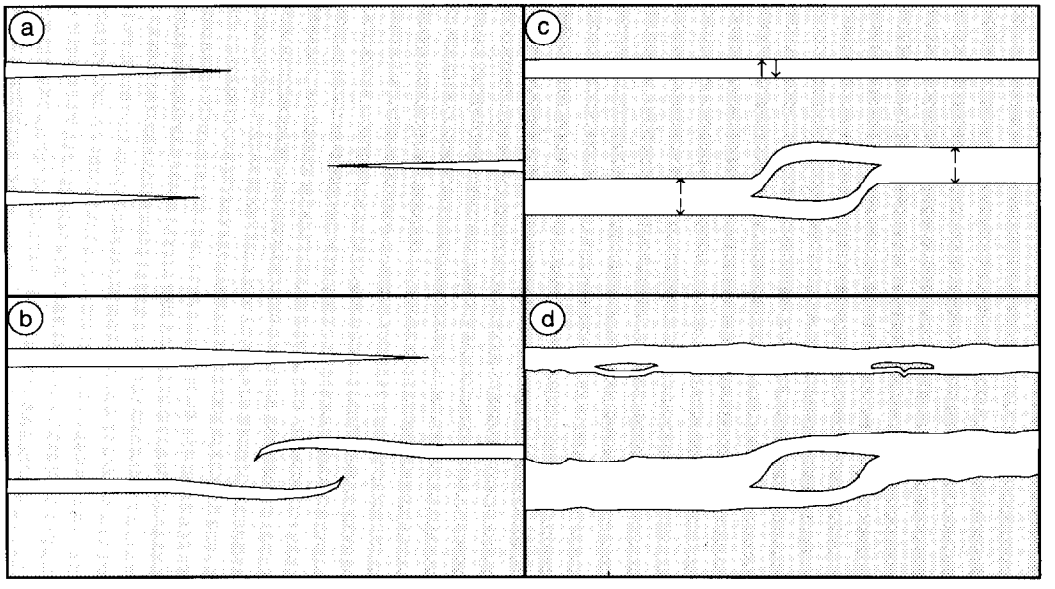

Fig. 6. Vein-parallel dilatancy model. Quartz ribbons are shown in white and the matrix in grey. (a) Layer-parallel fractures develop in the gneiss and attract mobilized silica. (b)–(d) The quartz-filled fractures propagate and some interact with each other to form an asymmetric inclusion.

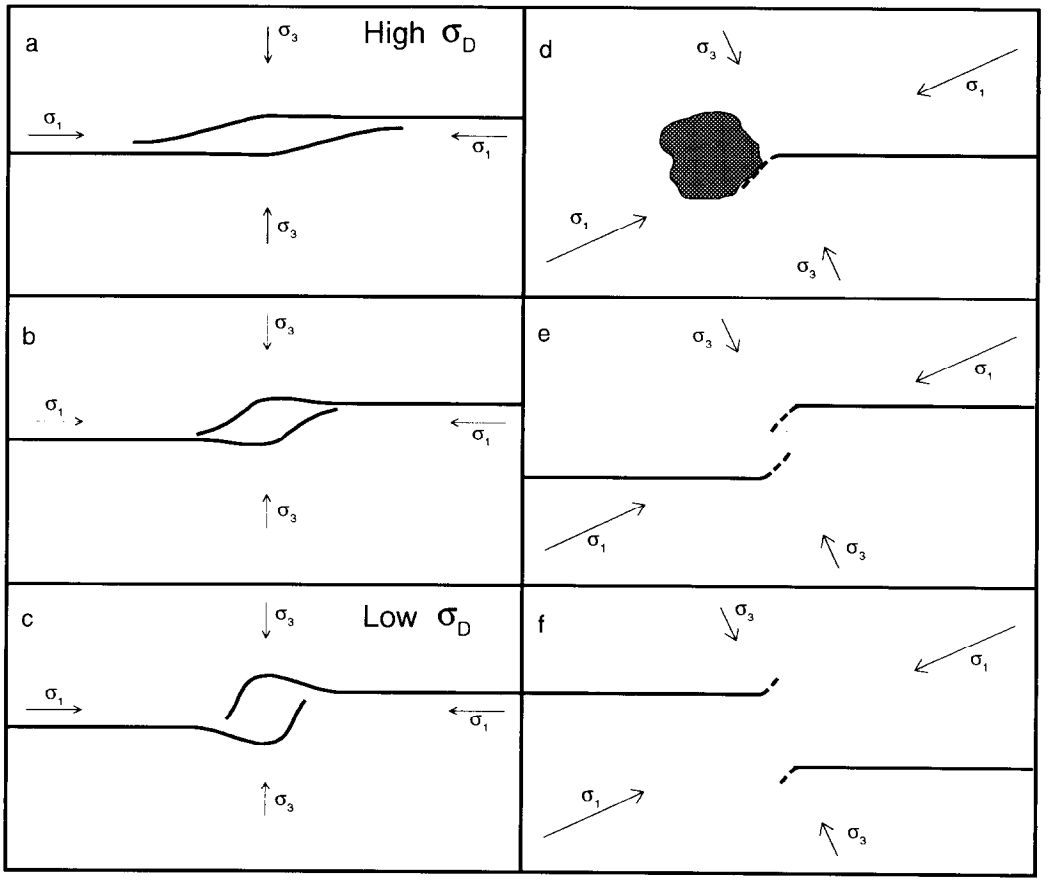

Fig. 7. Examples of asymmetric fracture propagation paths and crack interactions in a stress field. σ_1 is the maximum principal compressive stress. (a)–(c) The effect of crack interactions on the propagation and linking of two nearly co-planar fractures (Olson and Pollard, 1989). The progression from (a) to (c) represents decreasing stress difference and/or increasing crack interactions. (d) Fracture propagation around an obstacle such as a competent porphyroclast leads to a preferred direction of propagation in a left-lateral (this diagram) stress field. (e) Propagation of two left-stepping fractures in a left-lateral stress field leading to linking of the fractures. (f) Propagation of two right-stepping fractures in left-lateral stress field leading to non-linking of the fractures.

(Rogers and Bird, 1986, their fig. 5, Fig. 6 c–d). The second origin in which lenses of wallrock peeled and isolated during the joining of parallel quartz ribbons (Fig. 6c–d) is similar to the mechanism by which crack–seal veins include pieces of wallrock as they form (Ramsay, 1980; Ramsay and Huber, 1983, figs 13.25 and 13.35).

Ribbon inclusions and their symmetry can be interpreted in terms of fracture mechanics and fracture propagation theory. Pollard *et al.* (1982) have shown that mechanical interactions between parallel and adjacent dilatant cracks inhibit them from growing together tip-to-tip even if their offset is small. Local shear stresses at the fracture tips promote divergent rather than convergent propagation of the fractures (Olson and Pollard, 1989). As fracture overlap increases, the fracture propagation paths become more curved and fractures link with tip-to-plane intersections (Fig. 7a–c). In a stress field symmetric about the foliation plane the shape of the inclusion depends on the magnitude of the stress difference. The higher the stress difference, the greater the aspect ratio of the inclusion will be. No consistent asymmetry of the shape of the inclusion would form in such a stress field.

The interaction of two fractures propagating in an asymmetric stress field with principal directions σ_1 and σ_3 inclined to the foliation (Fig. 7e–f) (Segall and Pollard, 1980) can account for the consistent asymmetries observed here (Fig. 1a & f–h). As the fractures interact, they will tend to propagate towards the σ_1 direction. Depending on their relative position they will thus have a tendency to link, resulting in an inclusion (Fig. 7e), or to diverge (Fig. 7f) (Segall and Pollard, 1980). Similarly, a fracture propagating around an obstacle will also propagate into an orientation closer to the σ_1 direction (Pollard *et al.*, 1982) (Fig. 7d). Fractures may thus produce an asymmetric structure of ribbons diverging around rigid obstacles (Fig. 4). Asymmetries of ribbon terminations can therefore provide a shear sense indicator (Figs 3c & 4).

Vein-perpendicular dilatancy

In a second model, vein growth takes place by a mechanism called 'vein-perpendicular dilatancy' (Sawyer and Robin, 1986) (Fig. 8). Irregularities in a fracture surface lead to the development of small dilatant step fractures oriented approximately perpendicular to the layering and opening up in the direction parallel to the foliation plane with a component of shear along the foliation plane (Fig. 8a–b) (Sawyer and Robin, 1986). Veins grow by accretion along interfaces which are approximately perpendicular to the final ribbon morphology (Fig. 8c) hence the term vein-perpendicular dilatancy. Asymmetric inclusions can result from the development of a second dilatant step fracture parallel to the first (Fig. 8c–d).

Vein-perpendicular dilatancy requires a large component of slip along the ribbon interface to produce sufficient accretion of the ribbon. This large slip may lead to room accommodation problems at the ribbon tips. The blunt terminations of the ribbons suggest very little foliation-parallel slip at the ribbon tips. Although vein-parallel dilatancy seems more likely, there is no reason why a hybrid of the two models could not occur.

DISCUSSION

Fracturing in gneisses at high temperatures

That elastic fractures are possible in a ductile material when the strain rate is sufficiently high is demonstrated by the existence of pseudotachylites in high grade rocks (Clarke and Norman, 1993) and by the well known ability of silicone putty to fracture at high strain rates. We envisage our fractures to propagate through a creeping solid as shown schematically in Fig. 9.

No buckling of detached wallrock slivers within ribbons or of wallrock layers between ribbons is observed. We interpret this to imply that fracturing is most likely episodic and that only a few fractures are open in a given volume of rock at any one time (Fig. 9). Earlier formed fractures are healed prior to the propagation of a later one (Fig. 9) and behave as wallrock during the propagation of the next fracture (Ramsay, 1980). Slivers or wallrock layers therefore do not buckle because they may only be bordered by one active fracture at any one time. Mechanical interaction between fractures can only occur if both are active at the same time. Alternatively, what appears in section to be two separate interacting fractures may be in fact a single fracture bifurcating as it propagates around a local heterogeneity.

Role of fluids

Minor retrogression of K-feldspar to sericite is evidence that some H_2O-bearing fluids must have been present. Fluids are expected to have a significant effect on rheology and fracture properties of the rock. Fluid pressure may inhibit brittle behaviour by decreasing the creep strength of the rock through hydrolytic weakening or reaction softening (Gilotti, 1989). On the other hand fluid pressure can enhance brittle behaviour by lowering effective pressure (Ramsay and Huber, 1983) and through stress corrosion cracking (Atkinson and Meredith, 1987). Fluids may also have played an important role in the transport of silica by enhancing its transfer rate.

Source of silica

The silica for the ribbons may be local or external. Two different local sources may be envisaged. Some quartz can be produced by the metamorphic reactions responsible for the observed retrogressions. In the Huntsville gneisses, the replacement of orthopyroxene by biotite can be modelled as:

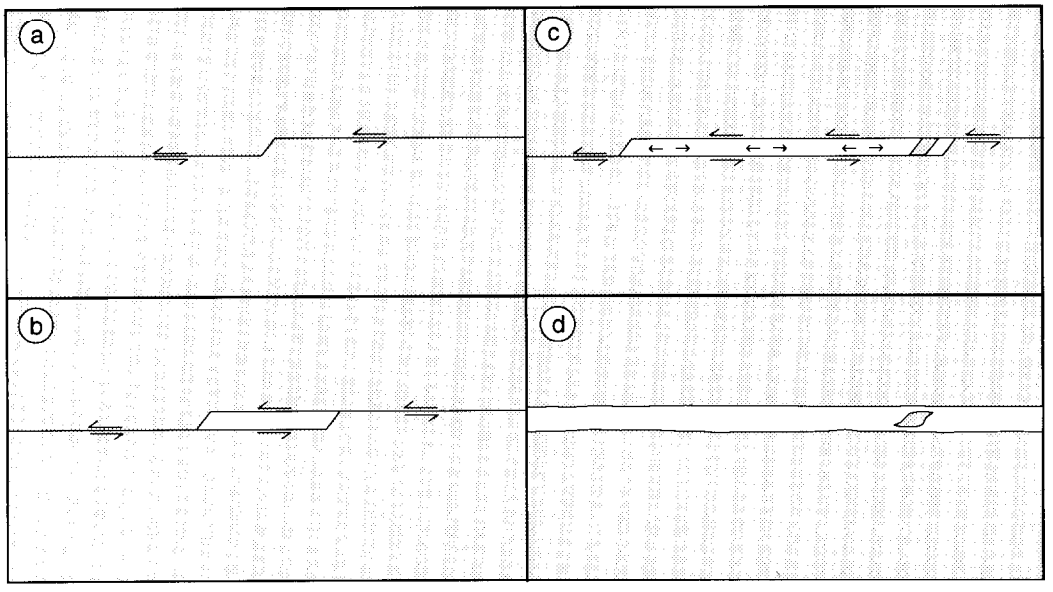

Fig. 8. Vein-perpendicular dilatancy model. (a) A layer-parallel fracture develops which has a local irregularity. (b) Slip along the irregular fracture surfaces creates a dilatant zone that attracts silica. (c) The vein grows by accretion along incipient fractures that are approximately perpendicular to the ribbon length. The growing vein may break off an asymmetric fragment of wall rock and include it in the vein as shown at the right edge of the vein. (d) A drawing of the quartz ribbon structure that may develop from this model.

$$5\ (Fe, Mg)_{2.4}Ca_{0.6}Al_2[Si_3O_{12}]$$
garnet

$$+\ 5\ (Mg, Fe)_2[Si_2O_6] + 8\ K[AlSi_3O_8] + 8\ H_2O$$
orthopyroxene K-feldspar

$$\rightarrow\ 21\ SiO_2 + 4\ K_2(Mg, Fe)_{5.5}Al_{0.5}[Si_{5.5}Al_{2.5}](OH)_4$$
quartz (1) biotite(2.6)

$$+\ 1\ Ca[Al_2Si_2O_8]$$
plagioclase (0.2)

In this and following reactions, numbers in parentheses behind the names of the product phases are volume fractions of the phases produced by the reaction, normalized to that of quartz.

In the CMBbtz, hydration of the feldspars, corrosion of orthpyroxenes, and formation of calcite can be accounted for by model reactions such as

$$4\ (Mg, Fe)_2[Si_2O_6] + 3K[AlSi_3O_8]$$
orthopyroxene K-feldspar

$$+\ 4\ Ca[Al_2Si_2O_8] + 4\ H_2O$$
plagioclase

$$\rightarrow\ 6\ SiO_2 + 4\ K_2Al_4[Si_6Al_2O_{20}](OH)_4$$
quartz (1) muscovite (6.2)

$$+\ 2\ Ca_2(Mg, Fe)_4Al[Si_7AlO_{22}](OH)_2$$
hornblende (4.1)

and

$$2\ K[AlSi_3O_8] + 2\ Ca[Al_2Si_2O_8] + 2\ H_2O + 2\ CO_2$$
K-feldspar plagioclase

$$\rightarrow\ 4\ SiO_2 + 1\ K_2Al_4[Si_6Al_2(OH)_4 +$$
quartz (1) muscovite (2.3)

$$+\ 2\ CaCO_3$$
calcite (0.4)

If most of the quartz observed in the ribbons were produced by these reactions, the modal fractions of the other products would have to be much larger than those observed in the rock. Other sources of silica must therefore be considered. Quartz may be derived locally through mobilization of silica along grain boundaries under high normal stress. The migration of silica would then be driven by variations in normal stress on boundaries, as argued by Ramsay (1980) for silica filling crack seal veins. In both cases of local derivation, the transport of silica occurs by H_2O-catalysed diffusion along grain boundaries.

Externally derived silica may be deposited by a fluid circulating through the rock along a network of opening fractures. In this model the distances travelled by the fluid and the silica can be greater than those permitted by grain boundary diffusion.

Scalloping of grain boundaries

Scalloping at grain boundaries is prominently displayed along the CMBbtz ribbons. The scallops are always convex towards the ribbon side (Figs 1f–h and

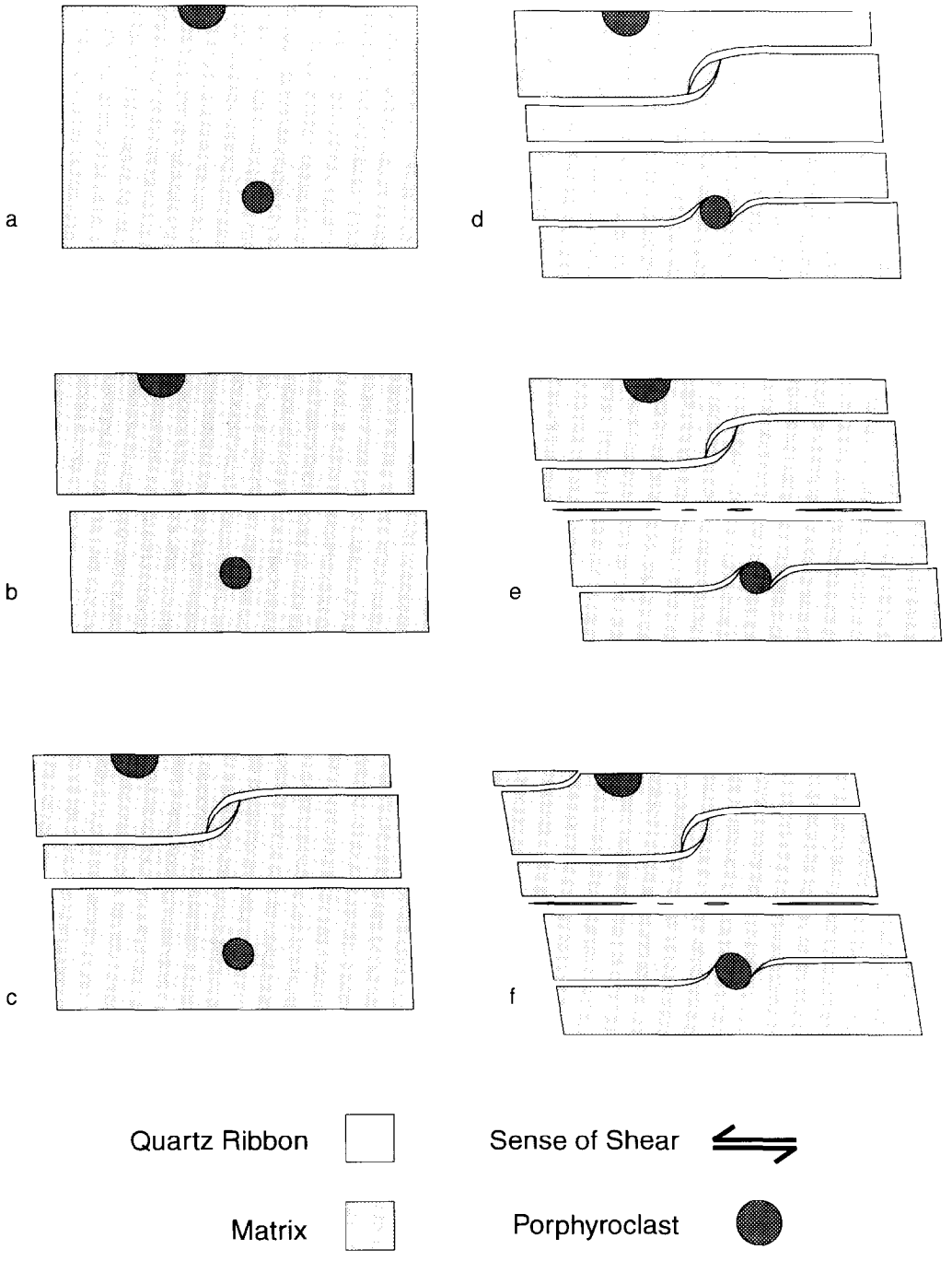

Fig. 9. Stepwise development of quartz-filled fractures within a shearing host rock. Only one or two fractures are active at any one time, but the host rock creeps continuously. (a) Prior to the formation of the fractures, the host rock has a strong horizontal foliation (not shown). (b) A first fracture propagates straight across the field of view along a foliation plane. (c) A second set of fractures propagate and link to isolate an asymmetric inclusion while the first fracture is inactive. (d) A third set of fractures are deflected asymmetrically around a porphyroclast. (e) Another fracture propagates along the edge of the first one isolating slivers of the host rock. (f) The rock continues to creep while a last fracture is deflected around a porphyroclast.

3b), and the observed ribbon walls therefore do not exactly coincide with the initial crack walls. Two possibilities can be envisaged for the scalloping. Both call upon the influence of surface energy and are not mutually exclusive:

(1) Reduction of surface energy results in a partial move towards the expected *Y*-shaped triple junctions between grains (Kretz, 1966; Vernon, 1968, 1970). Dihedral angles of close to 120° are observed in the matrix away from the ribbons (Fig. 1f).

(2) Erosion by metamorphic reactions mentioned above, with higher rates along grain–grain contacts again because of surface energy.The absence of scalloping in the Huntsville ribbons may suggest that these ribbons have not had the opportunity to reduce surface energy.

The effect of strain

A strong crystallographic preferred orientation in quartz ribbons is usually explained by rotation of glide systems during large strains (Wilson, 1975; Boullier and Bouchez, 1978). Boullier and Bouchez (1978) use the presence of a strong preferred crystallographic orientation to argue for large strains. Lister *et al.* (1978) demonstrate that 30 % of strain is required to develop a good crystallographic orientation in the absence of any recrystallisation. Such large strains are incompatible with our observations. However, many recent studies (Knipe and Law, 1987; Jessel, 1988) have shown that a strong crystallographic orientation can develop at small strains if recrystallization is active. Such recrystallization can produce large grains that are relatively free of defects (Fueten *et al.*, 1991).

A strong crystallographic orientation within large quartz grains in ribbons has also been attributed to annealing (secondary recrystallization) (Boullier and Bouchez's type B3) or metadynamic recrystallization (Culshaw and Fyson, 1984) of an earlier high strain texture. We suggest that extensive annealing required by these models is incompatible with the preservation of straight ribbon boundaries in the Huntsville gneisses and the thin inclusion slivers in all samples. The reduction of surface energy expected during extensive annealing would have eliminated straight boundaries and rounded the thin inclusions.

The fracture model for quartz ribbons accounts for the morphology of type B3 polycrystalline ribbons of Boullier and Bouchez (1978). However Boullier and Bouchez's (1978) types B1, B2 and B4 as well as Culshaw and Fyson's (1984) ribbons share many features with the ribbons described here such as straight boundaries and preserved inclusions (Gower and Simpson, 1992; Culshaw and Fyson, 1984). We propose that ribbons formed by fracturing and subsequently deformed under various conditions of strain rate and temperature can also produce Boullier and Bouchez's (1978) ribbon morphology types B1, B2 and B4.

Tectonic implications

The predominant regional deformation in both localities (Huntsville and CMBbtz) has been interpreted as northwest-directed thrusting during amphibolite to granulite facies metamorphism (Hanmer and McEachern, 1992; Nadeau and Hanmer, 1992). Late extensional shears of retrograde amphibolite facies assemblages crosscutting granulite grade rocks (Nadeau, 1991) have been documented in both the CGB and the CMBbtz; they are interpreted as warm collapse structures in the thrust-thickened (> 50 km) continental crust (Hanmer and McEachern, 1992; Hanmer, 1988a; Nadeau and Hanmer, 1992). A ductile orogenic extension of high-temperature (amphibolite-facies) which overprints earlier ductile thrusting has been documented in the Central Britt Shear Zone of the CGB (Culshaw *et al.*, 1994).

The asymmetries of the ribbons and inclusions are consistent with a south-side-down normal sense of shear. If the quartz ribbons formed during retrogressive metamorphism, as suggested by the scalloped texture of ribbon boundaries and the extreme mobility of silica, then they may have formed as part of a regional extensional shearing event. If this is the case, then a dominant textural feature of the gneisses, quartz ribbons, developed late in the deformation history by exploiting the anisotropy provided by the earlier regional thrust-developed gneissosity.

CONCLUSIONS

Quartz ribbons in straight gneisses of the southwestern Grenville Province exhibit straight ribbon boundaries, branching and feldspar promontories, lozenge-shaped and elongate ribbon inclusions, and consistent asymmetries of both ribbons and inclusions.

In the fracture model, quartz ribbons form as late synkinematic dilatant quartz-filled fractures along a strong pre-existing gneissosity. Little additional strain is required to produce ribbons by fracturing. Several sources of silica are possible: external origin, or local origin through stress-induced diffusion transfer or metamorphic reactions. The asymmetries of the quartz ribbons and ribbon-inclusions can be explained by interactions between fractures during their propagation and are consistent with a regional normal south-side-down sense of shear.

The ribbons described here are most similar in morphology to type B3 ribbons of Boullier and Bouchez (1978) which these authors interpreted as a result of large strains. The fracture model can explain ribbons of this type without requiring large strains. Under subsequent deformation at various strain rates and temperatures, ribbons of fracture origin could also evolve into the morphologies described by Boullier and Bouchez (1978) as types B1, B2, and B4; but such strains need not be large. An interpretation of ribbon origin thus has important implications for the strain history of the host rock.

Acknowledgements—The manuscript has greatly benefitted from reviews by S. Hanmer and A. Vauchez. The authors would also like to thank M. Lozon for his assistance with drafting the figures. This project was supported by Natural Sciences and Engineering Research Council operating grants to P.-Y. F. Robin and F. Fueten.

REFERENCES

Anovitz, L. M. and Essene, E. J. (1990) Thermobarometry and pressure–temperature paths in the Grenville Province of Ontario. *Journal of Petrology* **31**, 197–241.

Atkinson, B. K. and Meredith, P. G. (1987) The theory of subcritical crack growth with applications to minerals and rocks. In *Fracture Mechanics of Rock*, ed. B. K. Atkinson. Academic Press, London.

Bouchez, J.-L. (1977) Plastic deformation of quartzites at low temperature in an area of natural strain gradient. *Tectonophysics* **39**, 25–50.

Boullier, A.-M. and Bouchez, J.-L. (1978) Le quartz en rubans dans les mylonites. *Bulletin of the Geological Society, France* **7**, 253–262.

Clarke, G. L. and Norman, A. R. (1993) Generation of pseudotachylite under granulite facies conditions, and its preservation during cooling. *Journal of Metamorphic Geology* **11**, 319–335.

Culshaw, N. G. and Fyson, W. K. (1984) Quartz ribbons in high grade granite gneiss: modifications of dynamically formed quartz *c*-axis preferred orientation by oriented grain growth. *Journal of Structural Geology* **6**, 663–668.

Culshaw, N. G., Ketchum, J. W. F., Wodicka, N. and Wallace, P. (1994) Deep crustal extension following thrusting in the southwestern Grenville Province, Ontario. *Canadian Journal of Earth Science* **31**, 160–175.

Davidson, A., Culshaw, N. G. and Nadeau, L. (1982) A tectono-metamorphic framework for part of the Grenville Province, Parry Sound region, Ontario. In *Current Research, Geological Survey of Canada*, **Paper 82-1A**, 175–190.

Fueten, F., Robin, P.-Y. F. and Stephens, R. (1991) A model for the development of a domainal quartz *c*-axis fabric in a coarse-grained gneiss. *Journal of Structural Geology* **13**, 1111–1124.

Gilotti, J. A. (1989) Reaction progress during mylonitization of basaltic dikes along the Särv thrust, Swedish Caledonides. *Contributions to Mineral Petrology* **101**, 30–45.

Gower, R. J. W. and Simpson, C. (1992) Phase boundary mobility in naturally deformed, high-grade quartzofeldspathic rocks: evidence for diffusional creep. *Journal of Structural Geology* **14**, 301–313.

Hanmer, S. (1988a) Ductile thrusting at mid-crustal level, southwestern Grenville Province. *Canadian Journal of Earth Science* **25**, 1049–1059.

Hanmer, S. (1988b) Geology, western portion of the Central Metasedimentary Belt Boundary Zone, Grenville Province; parts of the Haliburton, Wilberforce, Kawagama Lake and Whitney map areas, Ontario. *Geological Survey of Canada, Open File* **1757**, 1:50,000.

Hanmer, S. and McEachern, S. (1992) Kinematical and rheological evolution of a crustal-scale ductile thrust zone, Central Metasedimentary Belt, Grenville orogen, Ontario. *Canadian Journal of Earth Science* **29**, 1779–1790.

Jessell, M. W. (1988) Simulation of fabric development in recrystallizing aggregates — II. Example model runs. *Journal of Structural Geology* **10**, 779–793.

Knipe, R. D. and Law, R. D. (1987) The influence of crystallographic orientation and grain boundary migration on microstructural and textural evolution in a *S–C* mylonite. *Tectonophysics* **135**, 155–169.

Kretz, R. (1966) Interpretation of the shape of mineral grains in metamorphic rocks. *Journal of Petrology* **7**, 68–94.

Lister, G. S., Paterson, M. S. and Hobbs, B. E. (1978) The simulation of fabric development in plastic deformation and its application to quartzite: the model. *Tectonophysics* **45**, 107–158.

MacKinnon, P. (1994) Deformation of Straight Gneisses: Rheological Modelling and Petrographic Analysis. Unpublished Ph.D. Thesis, University of Toronto.

Mancktelow, N. S. (1987) Atypical textures in quartz veins from the Simplon Fault zone. *Journal of Structural Geology* **9**, 995–1006.

McLelland, J. M. (1984) The origin of ribbon lineation within the southern Adirondacks, U.S.A. *Journal of Structural Geology* **6**, 147–157.

Moore, J. M. (1986) Introduction: the Grenville Problem then and now. In *The Grenville Province*, eds J. M. Moore, A. Davidson and J. A. Baer, Vol. **31**, pp. 1–12. Geological Association of Canada Special Paper.

Nadeau, L. (1991) Friends of the Grenville 1991 Field Trip Guidebook: Tectonic evolution of the Central Gneiss Belt, Huntsville area, Ontario. *1991 FOG Field Trip Meeting*.

Nadeau, L. and Hanmer, S. (1992) Deep-crustal break-back stacking and slow exhumation of the continental footwall beneath a thrusted marginal basin, Grenville orogen, Canada. *Tectonophysics* **210**, 215–233.

Olson, J. and Pollard, D. D. (1989) Inferring paleostresses from natural fracture patterns: a new method. *Geology* **17**, 345–348.

Pollard, D. D., Segall, P. and Delaney, P. T. (1982) Formation and interpretation of dilatant echelon cracks. *Bulletin of the Geological Society, America* **93**, 1291–1303.

Ramsay, J. G. (1980) The crack–seal mechanism of rock deformation. *Nature* **284**, 135–139.

Ramsay, J. G. and Huber, M. I. (1983) *Modern Structural Geology*. Academic Press, New York.

Robin, P.-Y. F. and Jowett, C. E. (1986) Computerized density contouring and statistical evaluation of orientation data using counting circles and continuous weighting functions. *Tectonophysics* **121**, 207–223.

Rogers, R. D. and Bird, D. K. (1986) Fracture propagation associated with dike emplacement at the Skaergaard intrusion, East Greenland. *Journal of Structural Geology* **8**, 71–86.

Sawyer, E. W. and Robin, P.-Y. F. (1986) The subsolidus segregation of layer-parallel quartz–feldspar veins in greenschist to upper amphibolite facies metasediments. *Journal of Metamorphic Geology* **4**, 237–260.

Segall, P. and Pollard, D. D. (1980) Mechanics of Discontinuous Faults. *Journal of geophysical Research* **85**, 4337–4350.

Thomas, A. L. and Pollard, D. D. (1993) The geometry of echelon fractures in rock: implications from laboratory and numerical experiments. *Journal of Structural Geology* **15**, 323–334.

van Breemen, O. and Hanmer, S. (1986) Zircon morphology and U–Pb geochronology in active shear zones: studies on syntectonic intrusions along the NW boundary of the Central Metasedimentary Belt Grenville Province, Ontario. In *Current Research, Part B, Geological Survey of Canada*, **Paper 86-1B**, 775–784.

Vauchez, A. (1980) Ribbon texture and deformation mechanisms of quartz in a mylonitized granite of Great Kabylia (Algeria). *Tectonophysics* **67**, 1–12.

Vernon, R. H. (1968) Microstructures of high-grade metamorphic rocks at Broken Hill, Australia. *Journal of Petrology* **9**, 1–22.

Vernon, R. H. (1970) Comparative grain-boundary studies of some basic and ultrabasic granulites, nodules and cumulates. *Scottish Journal of Geology* **6**, 337–351.

Wilson, C. J. L. (1975) Preferred orientation in quartz ribbon mylonites. *Bulletin of the Geological Society, America* **86**, 968–974.